Exogenous 4-1BB co-stimulation enhances memory B cell response during malaria.

Carolina Caloba[1,2], Alexandria J. Sturtz[3,6], Akshaya Ramachandran[1,7], Lijo John[1,2], Kateryna Malkina[1,4], Allen M. Minns[5], Scott E. Lindner[5], Rahul Vijay[1,2]

[1]Center for Cancer Cell Biology, Immunology and Infection, [2]Department of Microbiology and Immunology, Rosalind Franklin University of Medicine and Science, North Chicago, IL, USA. [3]Department of Microbiology and Immunology, University of Iowa, Iowa City, Iowa, USA, [4]Lake Forest College, Lake Forest, Illinois, USA.[5]Department of Biochemistry and Molecular Biology, Hucks Center for Malaria Research, Pennsylvania State University, University Park, Pennsylvania, USA. [6]Current Address: Division of Biology and Biomedical Sciences, Washington University, St.Louis, Missouri, USA. [7]Current Address: Harvard Medical School, Boston, Massachusetts, USA

Running Title: 4-1BB stimulation and memory B cells

Abstract:

Clearance of the malarial parasite and protection from reinfection is dependent on T helper cell-dependent germinal center (GC) -derived plasma cells (PC) and memory B cells (MBC). Enhancing or blocking T cell help during experimental malaria has been shown to either improve or impede GC output, respectively. Using a mouse model of malaria, we show that an agonistic antibody against the co-stimulatory molecule, 4-1BB (CD137), hinders an optimal GC response, but enhances humoral immune memory. We demonstrate that this apparent paradox is at least partially driven by CD4 T cell-intrinsic *Eomesodermin* expression. By using chemoprophylaxis or irradiated parasites we show that the beneficial effects of 4-1BB ligation on humoral immune memory are neither influenced by the inflammatory milieu, nor due to an increased number of MBCs, but rather due to their heightened recall capacity and their ability to readily differentiate into antibody secreting PCs.

Introduction

Despite decades of research, malaria still remains a major public health threat with an estimated 247 million cases and 619000 related deaths in 2021(1). The burden of the disease is further exacerbated by *Plasmodium*-immune evasion strategies as well as the continuing emergence of drug-resistant strains. Humoral immune memory following *Plasmodium* exposure is suboptimal, resulting in repeat infections. While the approval of the anti-malarial vaccine RTS,S/AS01, to be used in children is a major breakthrough, it provides limited efficacy (~30%) even after the regimented 4 doses (2).

Clearance of the malarial parasite relies on spatially and temporally layered CD4 T cell-dependent B cell activation events culminating in the production of parasite-specific antibodies. Concomitant with the clearance of infection, a fraction of activated B cells differentiates into MBCs, that quickly become antibody-secreting PC upon reinfection. However, increasing evidence suggest that, while humoral immune memory against *Plasmodium* provides clinical immunity, sterilizing immunity is rarely achieved (3). Expression and engagement of coinhibitory receptors such as PD1, LAG3, and CTLA-4 on CD4 T cells have been attributed to this suboptimal anti-*Plasmodium* immune responses *(4-8)*. These studies used combinatorial approaches to simultaneously block the inhibitory receptors while also activating costimulatory molecule (such as OX-40) to improve both effector and humoral immune memory (4, 6, 7). Previous studies have reported that agonizing OX40, a member of the tumor necrosis factor receptor superfamily (TNFRSF) expressed on T cells would improve both effector and humoral immune memory following *Plasmodium* infection (6, 7). 4-1BB or CD137 is another TNFRSF member expressed on T cells whose precise role in modulating anti-*Plasmodium* immunity have not been explored.

In this study, we investigated the role of exogenous 4-1BB stimulation using a monoclonal antibody, 3H3, in a rodent malaria model and show an enhancement in memory B cell response (MBC). We show that while 3H3 treatment derails effector humoral immune response and early parasite control, it

significantly improves the humoral immune memory-mediated protection from an otherwise acutely lethal *Plasmodium* challenge.

Materials and Methods

Animals, infection, treatments and parasitemia

C57BL/6 mice wild-type were purchased from The Jackson Laboratory. *CD4*$^{Ert2\text{-}Cre}$ and *Eomes*$^{fl/fl}$ mice were obtained from Dr. Noah Butler (University of Iowa), and 4-1BB KO mice from Dr.Tania Watts (University of Toronto) and are bred in-house. *Plasmodium yoelli* (*Py*) clone 17XNL and *P. berghei* clone ANKA (*Pb.ANKA*) were obtained from the Malaria Research and Reference Reagent Resource Center (MR4; American Type Culture Collection), stocks generated and mice infected as previously described (9). *Py* -infected mice were treated intraperitoneally with either 50 μg of anti-4-1BB antibody (3H3; BioXCell) or Rat IgG (rIgG) on days 5 and 7 post infection. For *CD4* $^{Ert2\text{-}Cre}$*Eomes*$^{fl/fl}$ experiments, 4 mg of tamoxifen (TAM) (Sigma, MO) were administered intraperitoneally on days 2, 3 and 4 post infection. In some experiments, mice were treated with either 100 μL of Artemether (10mg/mL) or Mineral Oil. Parasitemia was measured by flow cytometry as previously described.(10, 11). All experiments and procedures were approved by the Rosalind Franklin University of Medicine and Science Institutional Animal Care and Use Committee.

Confocal imaging

Spleens were processed as previously describedn(9). Antibodies used for staining are B220-AF488 (clone RA3-6B2; eBioscience), CD4-AF594 (clone GK1.5; BioLegend) and GL7-AF647 (BD Pharmingen). Imaging was done using a Zeiss LSM710 confocal microscope and images were processed using IMARIS x64 software (version 9.2.1).

ELISpot and ELISA

Nunc MaxiSorp white polystyrene plates were coated with 0.5 μg ml^{-1} of recombinant MSP1$_{19}$ and blocked for at least 2 h with PBS + 2.5% w/v BSA + 5% v/v goat serum. Bone marrow cells from *P. berghei* ANKA-infected mice were serially diluted in supplemented Iscoves modified Dulbecco's media and plated for 20 h at 37 °C with 5% CO_2. Plates were washed with PBS + 0.05% Tween 20 and incubated overnight with horseradish peroxidase (HRP)-conjugated IgM at 4 °C. Spots were developed with 3-amino-9-ethylcarbazole**.**

Nunc MaxiSorp plates were coated with 0.5 μg ml^{-1} MSP1$_{19}$ and blocked with 2.5% w/v BSA + 5% v/v normal goat serum. Serum samples from naive and *Py*-infected mice were serially diluted and incubated for 18 h at 4 °C. MSP1$_{19}$-specific antibodies were detected with HRP-conjugated IgG2b or IgG2c. Plates were developed using a SureBlue reserve TMB Kit (KPL), according to the manufacturer's protocol, and absorbance was measured at an optical density of 450 nm using a SpectraMax 340 (Molecular Devices). End-point titers were extrapolated from a sigmoidal 4PL (where x is the log concentration) standard curve for each sample. The threshold for end-point titers was the mean plus 0.5–8 multiplied by the standard deviation recorded for naive mouse sera.

Flow cytometry

After generation of single-cell suspension of splenocytes, RBCs were lysed and the cells were counted. Samples were blocked using Fc block (clone 2.4G2) in FACS buffer (PBS + 0.09% w/v sodium azide + 2% v/v fetal calf serum) and cells were stained with fluorescently labeled antibodies. Transcription factors were stained using Foxp3 Transcription factor staining buffer (Tonbo), according to manufacturer's protocol. Samples were acquired on BD-LSR-II or Cytek Aurora and analyzed using FlowJo software (TreeStar Inc).

SpyCage Reagent for detecting MSP1$_{-19}$ specific B cells

SpyCage reagents bearing 60 copies of either mScarlet ("RedCage") or mNeonGreen ("GreenCage") were covalently loaded with 60 copies of the immunodominant *P. yoelii* antigen MSP1 or the liver stage antigen PyUIS4 as a decoy control, respectively. Antibodies specific to SpyCage were biotinylated using amine-reactive biotinylated crosslinkers, and were used to enrich SpyCage-bound cells.

MBC transfer

Memory B cells (B220$^+$IgD$^-$CD38$^+$GL7$^-$) were sort-purified from *Py*-infected mice treated with rIgG or 3H3. 2x10^5 cells were transferred intravenously to naive μMT mice, which were infected with 1 × 10^6 *Py* -parasitized RBCs.

Statistical analysis

All statistical analyses were performed using GraphPad Prism 10 software (GraphPad). Specific tests are detailed in the figure legends.

Results and Discussion

Exogenous 4-1BB co-stimulation delays GC response

Our initial studies revealed ~2-3-fold higher numbers of 4-1BB$^+$ CD4 T cells compared to their CD8 T cell counterparts both in naïve as well as *Plasmodium yoelii* (*Py*) infected mice (up to 7 dpi) (**Supplemental Fig. 1*A***) and that 4-1BB KO mice infected with *Py* showed heightened parasite load compared to WT mice (**Fig. 1*A***). Enhanced susceptibility of KO mice was also associated with a significantly reduced GC response (data not shown). Notably, and contrary to the role of OX40 ligation(6), ligation of 4-1BB using an agonistic monoclonal antibody (Ab) (clone 3H3) showed a prolonged infection course with an 8-fold higher total parasite load, which eventually resolved by day 39-40 p.i. (**Fig. 1*B***). We next investigated whether delayed parasite control in 3H3-treated mice was associated with perturbations of GC-associated effector populations (**Supplemental Fig 1*B,C***). We found reduced frequencies and numbers of GC B cells (**Fig. 1*C***) and GC Tfh cells (**Fig. 1*D***) and serum-anti-*Plasmodium* antibody titers (**Fig.1 *E***) until at least day 39 post-infection (p.i). Concomitant with the delay in GC response, we also observed a pronounced disruption of lymphoid architecture following 3H3 treatment until 21 d.p.i (**Fig. 1*F***). However, by 39 d.p.i the follicles regrouped into GCs coinciding with the resolution of infection in 3H3-treated, *Plasmodium*-infected mice (**Fig. 1*F***). These data show that 4-1BB is necessary for optimal *Plasmodium* parasite control and that agonistic ligation of 4-1BB distorts lymphoid architecture and GC orchestration during experimental malaria.

Deletion of CD4-intrinsic Eomes rescues GC response following exogenous 4-1BB co-stimulation

3H3-mediated engagement of 4-1BB upregulates eomesodermin (EOMES) in CD4 T cells(12) which we also observed in *Plasmodium* infection-induced effector CD4 T cells by day 9 p.i (**Supplemental Fig. 2*A***). However, the number of EOMES$^+$ cells waned by day 21 p.i, which coincided with the appearance of BCL6$^+$ CD4 T cells in 3H3 treated mice (**Supplemental Fig. 2*B,C***). This observation led us to speculate that EOMES and BCL6 in CD4 T cells may counter-repress one another during *Py* infection. To test whether the lack of CD4 T cell- intrinsic *BCL6* facilitates EOMES upregulation, we infected *CD4.Cre.Bcl6$^{fl/fl}$* mice with *Py* and treated them with 3H3 or rIgG. 3H3 treatment resulted in EOMES upregulation independent of BCL6 expression, showing that BCL6 does not regulate EOMES expression (**Supplemental Fig. 2*D***). To test the converse notion of whether EOMES regulates BCL6 expression, we infected

CD4.Ert2.Cre.Eomes$^{fl/fl}$ mice with *Py*, followed by Tamoxifen (TAM) treatment to trigger deletion of EOMES in CD4 T cells (**Supplemental Fig. 2*E, left panel***). Deletion of EOMES in CD4 T cells neither affected the expression of BCL6 (**Supplemental Fig. 2*F)*** nor altered parasite control in *Py-CD4.Ert2.Cre.Eomes*$^{fl/fl}$ infected mice (**Supplemental Fig. 2*G)***. However, when EOMES in CD4 T cells was deleted in *Py*-infected mice (Cre^{+}) treated with 3H3, we observed a marked enhancement of parasite control compared to Cre^{-} mice (**Fig. 2*A***). This enhanced parasite control was associated with elevated numbers of GC B cells (**Fig. 2*B***) and GC Tfh cells (**Fig. 2*C***). Thus, no apparent counterregulatory loop exists between EOMES and BCL6, yet the detrimental effects of 3H3-mediated ligation of 4-1BB on GC responses requires CD4 T cell-intrinsic expression of EOMES.

Exogenous 4-1BB costimulation enhances survival following lethal Plasmodium challenge

A delayed effector GC response following 3H3 treatment (**Fig. 1**) is predicted to also impair protective humoral immune memory responses against a subsequent parasite challenge. To test this, we monitored survival and humoral immune memory responses in convalescent *Py*-infected-3H3/rIgG treated WT mice that were challenged (day 93 p.i) with a virulent and acutely lethal *Plasmodium* strain, *P. berghei ANKA (Pb.ANKA)*. We observed that 3H3-treated, convalescent mice showed significantly higher survival rates compared to rIgG-treated mice following *Pb.ANKA* challenge (**Fig. 3*A***). Enhanced survival of 3H3-treated mice correlated with greater fold increases in anti-merozoite surface protein (MSP1$_{-19}$)-specific antibody titers between day 0 and day 5 post-*Pb.ANKA* challenge (**Fig. 3*B***), a measure of enhanced memory B cell (MBC) recall response. Because derailed effector GC responses in 3H3-treated mice requires CD4 T cell-intrinsic *EOMES* expression (**Fig. 2**), we investigated whether EOMES expression also governs immune memory-mediated protection against heterologous *Pb.ANKA* challenge. *Py*-infected *CD4.Ert2.Cre.Eomes*$^{fl/fl}$ (Cre^{+}) mice and their genetic littermate control cohorts (Cre-) were treated with TAM on days 2-4 p.i followed by 3H3 on 5 and 7 dpi (as in **Fig. 2**) and subsequently challenged with *Pb.ANKA* on day 93 post-*Py* infection. We found that CD4 T cell-intrinsic expression of EOMES is also necessary for immune memory-mediated resistance to *Pb.ANKA* challenge (**Fig. 3C**). The loss of protection in *Cre*$^{+}$ mice strongly correlated with a significantly subdued MBC recall as evidenced by a lower fold increase in anti-MSP1$_{-19}$-specific antibody levels, compared to their *Cre*$^{-}$ littermates (**Fig. 3*D***). These data show that CD4 T cell-intrinsic EOMES expression is essential for enhanced MBC recall following 3H3 treatment.

To investigate whether the enhanced MBC recall and subsequent improvement in survival following 3H3 treatment (**Fig. 1*A***) is independent of the heightened inflammation that may ensue higher and prolonged parasite load (**Fig. 1*A***), we truncated infection in *Py*-infected, 3H3- or rIgG-treated WT mice by administering the antimalarial drug artemether on 12-14 dpi (**Supplemental Fig. 3*A***). Notably, compared to vehicle (mineral oil)-treated mice, artemether treatment neither compromised protection (**Fig. 3*E***) nor impaired the enhanced MBC recall response (**Fig. 3*F***) mediated by 3H3 treatment following *Pb.ANKA* challenge. Notably, artemether treatment did not alter EOMES expression in CD4 T cells (**Supplemental Fig. 3*B***), and did not rescue the effector (day 21 p.i.) GC responses in *Py* infected 3H3-treated mice (**Supplemental Fig. 3*B,C***), which matched infection outcomes in mice treated with 3H3 alone *(***Supplemental Fig. 2*A)***. To test whether 3H3-mediated enhanced immune memory protection is relevant to attenuated *Plasmodium* parasite vaccination, we immunized mice with irradiated blood stage *Py* parasites and subsequently administered either 3H3 or rIgG on days 5 and 7 p.i. On day 30 p.i, vaccinated mice were challenged with *Pb.ANKA* and we observed superior protection and MBC recall in 3H3-treated, radiation attenuated parasite vaccinated mice (**Fig. 3*G,H***), which aligns with our results in mice infected with live *Py* parasites. Collectively, our data reveal a critical pathway that enhances both infection- and vaccination-induced MBC recall responses following exogenous 4-1BB stimulation.

Enhanced immune memory responses following 4-1BB ligation are MBC-intrinsic

Pathogenic infections or vaccinations typically establish GC-driven protective immune memory responses that are mediated by the presence and function of MBCs and plasma cells (PC)(13). The elevated class-switched, parasite-specific antibody titers measured between d0 and d5 p.i following *Pb.ANKA* challenge (**Fig. 3**) in 3H3-treated mice is suggestive of an enhanced memory response that may result from either an elevated number of MBCs or an enhanced differentiation capability of MBCs, both of which will result in larger number of antibody secreting PCs. Enumeration of splenic MBCs showed a significantly reduced number of both polyclonal (**Fig. 4*A, B)*** and antigen ($MSP1_{-19}$) specific fractions (**Fig. 4*C, D)*** in *Py*-infected 3H3- treated mice, compared to controls on 90 dpi. Further characterization of these MBCs based on CD73, CD80 and PDL2(14, 15) also revealed that 3H3-treated mice harbored significantly lower numbers of each of these subsets compared to control mice (**Supplemental Fig. 4*A-F***). Despite the lower steady state numbers of MBC in 3H3-treated mice, we observed that there was a significantly larger number of antibody secreting PCs in the bone marrow following *Pb.ANKA* challenge (**Fig. 4*E*),** suggesting that MBCs from 3H3-treated mice have a superior per-cell recall potential compared to MBC in rIgG-treated mice. To directly test the per-cell protective and functional capacity of both MBC populations, we flow-sorted MBCs from 3H3 or rIgG-treated mice and transferred an equal number into separate groups of B cell deficient (μMT) mice that were infected with *Py* the following day. We observed that *Py*-infected μMT mice that received MBCs from 3H3-treated donor mice exhibited lower parasite load compared to those receiving MBCs from rIgG-treated donor mice (**Fig. 4*F***), which further correlated with higher serum antibody titers (**Fig. 4*G***). These data collectively show that MBCs derived from 3H3-treated mice exhibit intrinsically superior function and capacity to differentiate into PCs that can mediate protection against *Plasmodium* challenge.

In this study we report that exogenous 4-1BB ligation during primary *Plasmodium* infection while derailing early GC responses, enhances humoral immune memory during experimental malaria. These data are in contrast to the paradigm that the quality of the effector GC response predicts the subsequent memory response. We show that that the beneficial effects of 4-1BB ligation (enhancement of memory response) are independent of the early parasite burden and inflammatory milieu that follows. Our experiments suggests that 4-1BB expression on CD4 T cells is required for this enhanced protection (*unpublished observations, Caloba and Vijay*) and that it is at least partially contributed by CD4 T cell-intrinsic EOMES expression (**Fig. 3*B, C***). Our observation that 3H3-treated mice begin with fewer MBCs of all subtype s (**Supplemental Fig. 4*A-F***), but do differentiate into greater number of antibody-secreting PCs upon antigen reexposure, strengthens our prediction that exogenous 4-1BB stimulation imprints a superior MBC program on B cells. In summary we show that despite a delayed and rather inefficient effector immune response, exogenous 4-1BB stimulation has the potential to enhance humoral immune memory in a CD4 T cell dependent manner. Our findings reported here are especially relevant in the context of the anti-malarial vaccine, RTS,S which currently offers only limited efficacy (~30%)(2). The possibility of using such an immunomodulatory approach following vaccination may enhance immunogenicity and overall efficacy of the vaccine.

References

1. WHO. World malaria report 2022. Geneva: World Health Organization;2022.
2. Laurens, M. B. 2020. RTS,S/AS01 vaccine (Mosquirix): an overview. *Hum Vaccin Immunother* 16: 480-489.
3. Tran, T. M., S. Li, S. Doumbo, D. Doumtabe, C. Y. Huang, S. Dia, A. Bathily, J. Sangala, Y. Kone, A. Traore, M. Niangaly, C. Dara, K. Kayentao, A. Ongoiba, O. K. Doumbo, B. Traore, and P. D. Crompton. 2013. An intensive longitudinal cohort study of Malian children and adults reveals no evidence of acquired immunity to Plasmodium falciparum infection. *Clin Infect Dis* 57: 40-47.
4. Butler, N. S., J. Moebius, L. L. Pewe, B. Traore, O. K. Doumbo, L. T. Tygrett, T. J. Waldschmidt, P. D. Crompton, and J. T. Harty. 2011. Therapeutic blockade of PD-L1 and LAG-3 rapidly clears established blood-stage Plasmodium infection. *Nat Immunol* 13: 188-195.
5. Kurup, S. P., N. Obeng-Adjei, S. M. Anthony, B. Traore, O. K. Doumbo, N. S. Butler, P. D. Crompton, and J. T. Harty. 2017. Regulatory T cells impede acute and long-term immunity to blood-stage malaria through CTLA-4. *Nat Med* 23: 1220-1225.
6. Zander, R. A., N. Obeng-Adjei, J. J. Guthmiller, D. I. Kulu, J. Li, A. Ongoiba, B. Traore, P. D. Crompton, and N. S. Butler. 2015. PD-1 Co-inhibitory and OX40 Co-stimulatory Crosstalk Regulates Helper T Cell Differentiation and Anti-Plasmodium Humoral Immunity. *Cell Host Microbe* 17: 628-641.
7. Zander, R. A., R. Vijay, A. D. Pack, J. J. Guthmiller, A. C. Graham, S. E. Lindner, A. M. Vaughan, S. H. I. Kappe, and N. S. Butler. 2017. Th1-like Plasmodium-Specific Memory CD4(+) T Cells Support Humoral Immunity. *Cell Rep* 21: 1839-1852.
8. Illingworth, J., N. S. Butler, S. Roetynck, J. Mwacharo, S. K. Pierce, P. Bejon, P. D. Crompton, K. Marsh, and F. M. Ndungu. 2013. Chronic exposure to Plasmodium falciparum is associated with phenotypic evidence of B and T cell exhaustion. *Journal of immunology* 190: 1038-1047.
9. Vijay, R., J. J. Guthmiller, A. J. Sturtz, F. A. Surette, K. J. Rogers, R. R. Sompallae, F. Li, R. L. Pope, J. A. Chan, F. de Labastida Rivera, D. Andrew, L. Webb, W. J. Maury, H. H. Xue, C. R. Engwerda, J. S. McCarthy, M. J. Boyle, and N. S. Butler. 2020. Infection-induced plasmablasts are a nutrient sink that impairs humoral immunity to malaria. *Nat Immunol* 21: 790-801.
10. Malleret, B., C. Claser, A. S. Ong, R. Suwanarusk, K. Sriprawat, S. W. Howland, B. Russell, F. Nosten, and L. Renia. 2011. A rapid and robust tri-color flow cytometry assay for monitoring malaria parasite development. *Sci Rep* 1: 118.
11. Villarino, N. F., G. R. LeCleir, J. E. Denny, S. P. Dearth, C. L. Harding, S. S. Sloan, J. L. Gribble, S. R. Campagna, S. W. Wilhelm, and N. W. Schmidt. 2016. Composition of the gut microbiota modulates the severity of malaria. *Proc Natl Acad Sci U S A* 113: 2235-2240.
12. Curran, M. A., T. L. Geiger, W. Montalvo, M. Kim, S. L. Reiner, A. Al-Shamkhani, J. C. Sun, and J. P. Allison. 2013. Systemic 4-1BB activation induces a novel T cell phenotype driven by high expression of Eomesodermin. *The Journal of experimental medicine* 210: 743-755.
13. Dhenni, R., and T. G. Phan. 2020. The geography of memory B cell reactivation in vaccine-induced immunity and in autoimmune disease relapses. *Immunol Rev* 296: 62-86.
14. Brown, S. L., J. J. Bauer, J. Lee, E. Ntirandekura, and J. S. Stumhofer. 2022. IgM(+) and IgM(-) memory B cells represent heterogeneous populations capable of producing class-switched antibodies and germinal center B cells upon rechallenge with P. yoelii. *Journal of leukocyte biology* 112: 1115-1135.
15. Zuccarino-Catania, G. V., S. Sadanand, F. J. Weisel, M. M. Tomayko, H. Meng, S. H. Kleinstein, K. L. Good-Jacobson, and M. J. Shlomchik. 2014. CD80 and PD-L2 define functionally distinct memory B cell subsets that are independent of antibody isotype. *Nat Immunol* 15: 631-637.

288 **FIGURE LEGENDS**
289
290 **FIGURE 1.** Exogenous 4-1BB co-stimulation delays GC response. *A*, WT or 4-1BB KO mice were infected
291 with $1x10^6$ *Py*-parasitized RBCs. Parasitemia was measured by flow cytometry on indicated timepoints
292 (n=5/group). *B-F*, WT mice were infected $1x10^6$ *Py*-parasitized RBCs and treated with 50µg of 3H3 or rIgG
293 on days 5 and 7 p.i. Parasitemia (*B, n=6*/group), splenic GC B cells (*C, n=3*/group), GC-Tfh cells (*D,*
294 *n=3*/group) was measured on indicated time points using flow cytometry and anti-$MSP1_{-19}$ IgG2b antibody
295 titers were measured by ELISA (*E*) and splenic GCs were visualized using confocal microscopy on
296 indicated timepoints (*F*). *A-D* – 2-way ANOVA and *E*, Student's *t* test used. All experiments are
297 representative of at least two independent experiments.
298
299 **FIGURE 2.** Deletion of CD4-intrinsic *Eomes* rescues GC response following exogenous 4-1BB co-
300 stimulation. *A-C*, *CD4.Ert2.Cre.Eomes*$^{fl/fl}$ mice were infected with $1x10^6$ *Py*-parasitized RBCs and were
301 treated with 400µg of Tamoxifen orally on days 2-4 dpi and with 3H3 on 5 and 7 dpi. Parasite load (*A*),
302 splenic GC B cell (*B*) and GC Tfh cells (*C*) were evaluated on indicated time points using flow cytometry.
303 *A-C*, n=3 data pooled from two independent experiments, *Mann Whitney* test used.
304
305 **FIGURE 3.** Exogenous 4-1BB stimulation enhances survival following lethal challenge. WT (*A-B, E-F, G-*
306 *H*) or *CD4.Ert2.Cre.Eomes*$^{fl/fl}$ (*C-D*) mice were infected with $1x10^6$ *Py*-parasitized RBCs (*A-F*) or irradiated
307 $1x10^6$ *Py*-parasitized RBCs (*G-H)* were treated with 3H3 or rIgG as indicated on day 5 and 7 p.i.). Mice
308 in *C, D* were treated with 400µg of Tamoxifen orally on days 2-4 dpi and mice in *E, F* were treated with
309 100 µL of Artemether (10mg/mL) on 12-14 dpi. Mice were challenged with *Pb.ANKA* on indicated
310 timepoints and survival was monitored. Serum was collected on the day (d0) of *Pb.ANKA* challenge and 5
311 days after (d5) and ELISA was performed to measure change in antibody titers (*B, C, D, F* and *H*) as a
312 measure of MBC recall. Data pooled from (A-F and H) or representative of 2 independent experiments.
313 Kaplan Meyer survival (*A, C, E* and *G*) or paired *t* test (*B, D, F* and *H*) used.
314
315 **FIGURE 4.** Superior MBCs recall following exogenous 4-1BB stimulation. *A-E*, WT mice infected with
316 $1x10^6$ *Py*-parasitized RBCs were treated with 50µg of 3H3 or rIgG on 5 and 7 dpi. On 90 dpi, splenic
317 polyclonal (*A, B*) and antigen specific (*C, D*) MBCs were evaluated. *E*, different cohort of 3H3 or rIgG-
318 treated mice were challenged with *Pb.ANKA* and bone marrow plasma cell numbers were evaluated using
319 ELIspot assay. *F, G,* MBCs from 3H3 or rIgG-treated mice were flow sorted and transferred into mMT
320 mice, which were infected with *Py* the next day, and parasitemia (*F*) on 12 dpi and serum antibody titers
321 were measured using ELISA (*G*). Data are representative (*A-E*) or are pooled (*n=6*/group) from two
322 independent experiments. Mann Whitney test used.
323

Figure 1

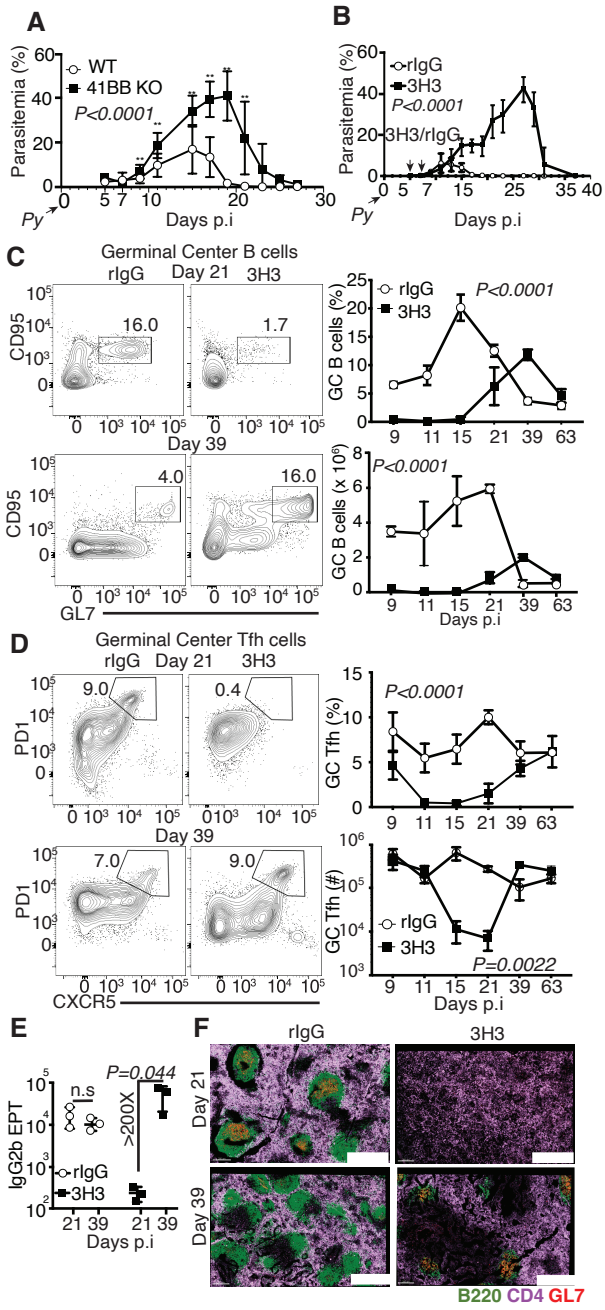
A
Parasitemia (%)
WT
41BB KO
P<0.0001
Py
Days p.i
B
Parasitemia (%)
rIgG
3H3
P<0.0001
3H3/rIgG
Py
Days p.i
C
Germinal Center B cells
rIgG
Day 21
3H3
CD95
16.0
1.7
Day 39
4.0
16.0
GL7
GC B cells (%)
P<0.0001
GC B cells (x 10^6)
P<0.0001
Days p.i
D
Germinal Center Tfh cells
rIgG
Day 21
3H3
PD1
9.0
0.4
Day 39
7.0
9.0
CXCR5
GC Tfh (%)
P<0.0001
GC Tfh (#)
P=0.0022
Days p.i
E
IgG2b EPT
n.s
P=0.044
>200X
rIgG
3H3
Days p.i
F
rIgG
3H3
Day 21
Day 39
B220 CD4 GL7

Figure 2

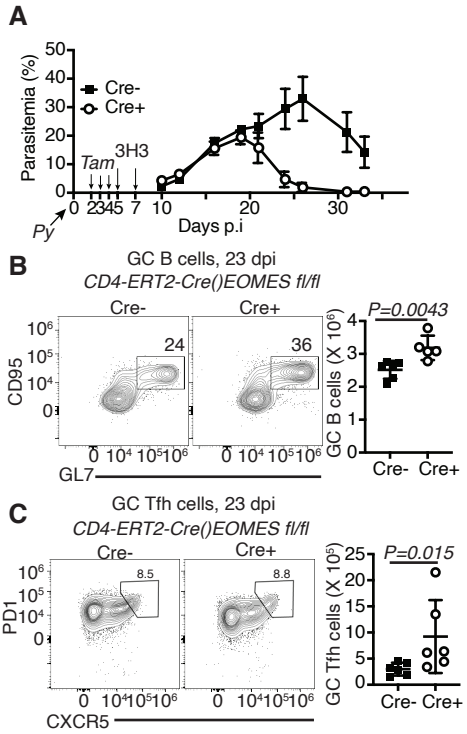
A
Parasitemia (%)
Cre-
Cre+
Tam
3H3
Py
Days p.i
B
GC B cells, 23 dpi
CD4-ERT2-Cre()EOMES fl/fl
Cre-
Cre+
24
36
CD95
GL7
P=0.0043
GC B cells (X 10^5)
C
GC Tfh cells, 23 dpi
CD4-ERT2-Cre()EOMES fl/fl
8.5
8.8
PD1
CXCR5
P=0.015
GC Tfh cells (X 10^5)

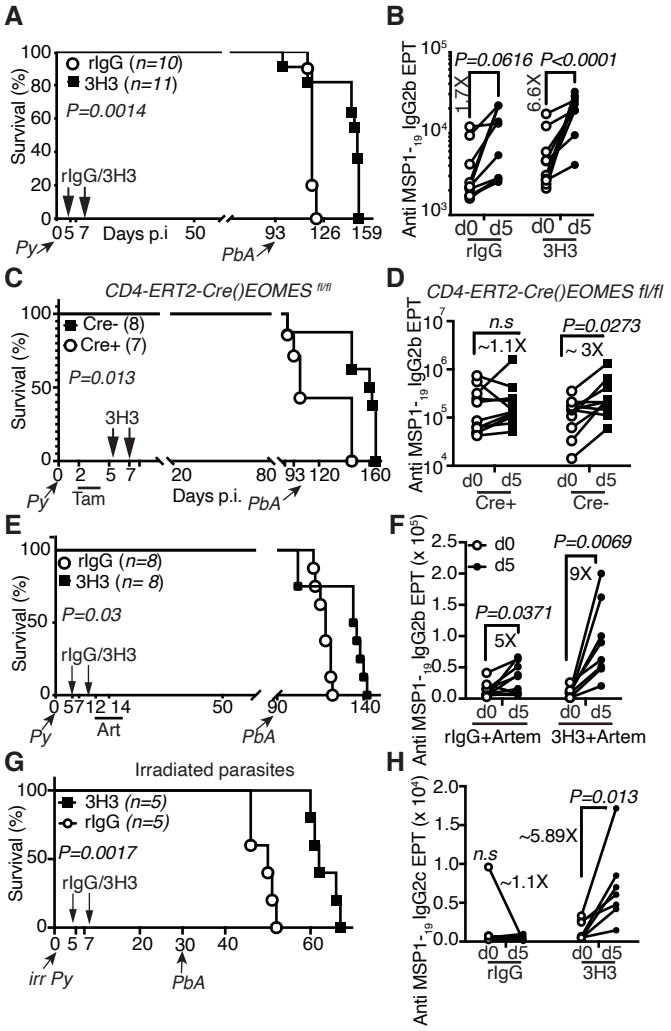
A
rIgG (n=10)
3H3 (n=11)
P=0.0014
Survival (%)
rIgG/3H3
Py
PbA
Days p.i
B
P=0.0616
P<0.0001
1.7X
6.6X
Anti MSP1-19 IgG2b EPT
d0 d5
rIgG
3H3
C
CD4-ERT2-Cre()EOMES fl/fl
Cre- (8)
Cre+ (7)
P=0.013
3H3
Tam
Days p.i.
D
CD4-ERT2-Cre()EOMES fl/fl
n.s
P=0.0273
~1.1X
~ 3X
Cre+
Cre-
E
rIgG (n=8)
3H3 (n= 8)
P=0.03
Art
F
d0
d5
P=0.0069
9X
P=0.0371
5X
rIgG+Artem
3H3+Artem
G
Irradiated parasites
3H3 (n=5)
rIgG (n=5)
P=0.0017
irr Py
H
P=0.013
~5.89X
n.s
~1.1X
Anti MSP1-19 IgG2c EPT (x 10⁴)

Figure 4

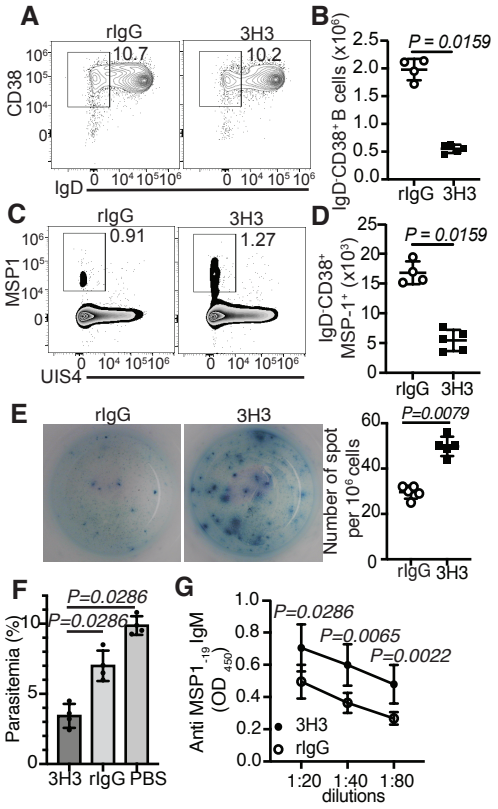
A
rIgG
3H3
10.7
10.2
CD38
IgD
B
P = 0.0159
IgD-CD38+ B cells (x10^6)
rIgG 3H3
C
rIgG
3H3
0.91
1.27
MSP1
UIS4
D
P = 0.0159
IgD-CD38+ MSP-1+ (x10^3)
rIgG 3H3
E
rIgG
3H3
P=0.0079
Number of spot per 10^6 cells
rIgG 3H3
F
P=0.0286
P=0.0286
Parasitemia (%)
3H3 rIgG PBS
G
P=0.0286
P=0.0065
P=0.0022
Anti MSP1-19 IgM (OD450)
3H3
rIgG
1:20 1:40 1:80
dilutions

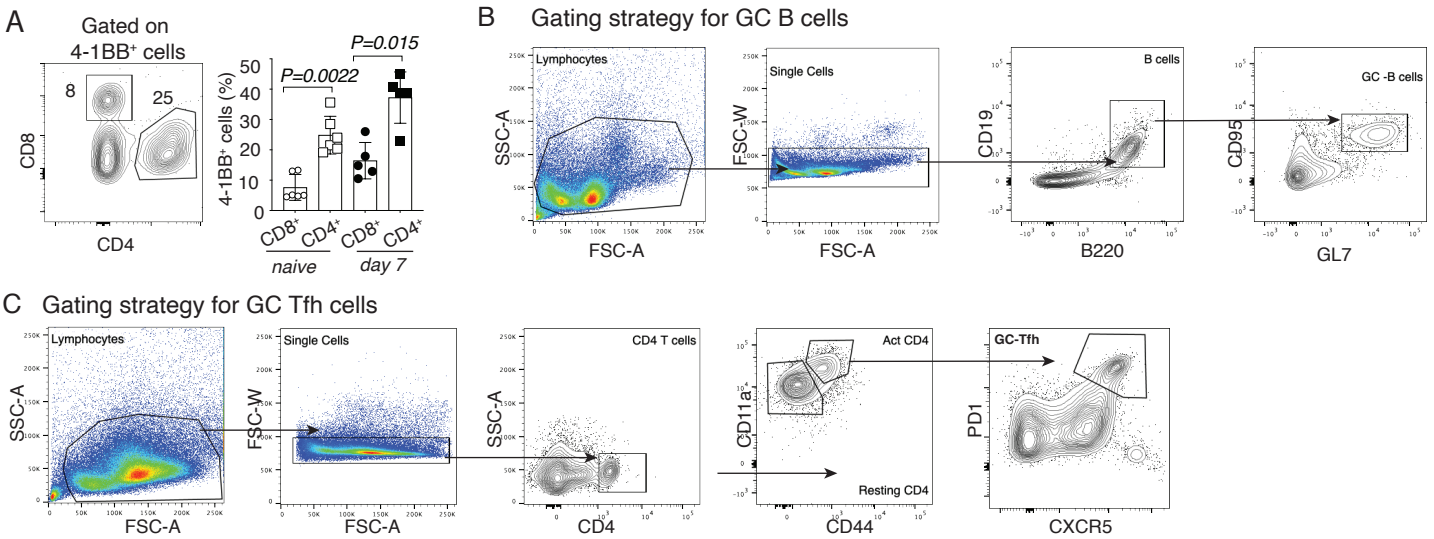

SUPPLEMENTAL FIGURE 1. A, Relative frequency of CD4 and CD8 T cell that express 4-1BB. Gating strategy for GC B cells (B) and GC-Tfh (C) shown.

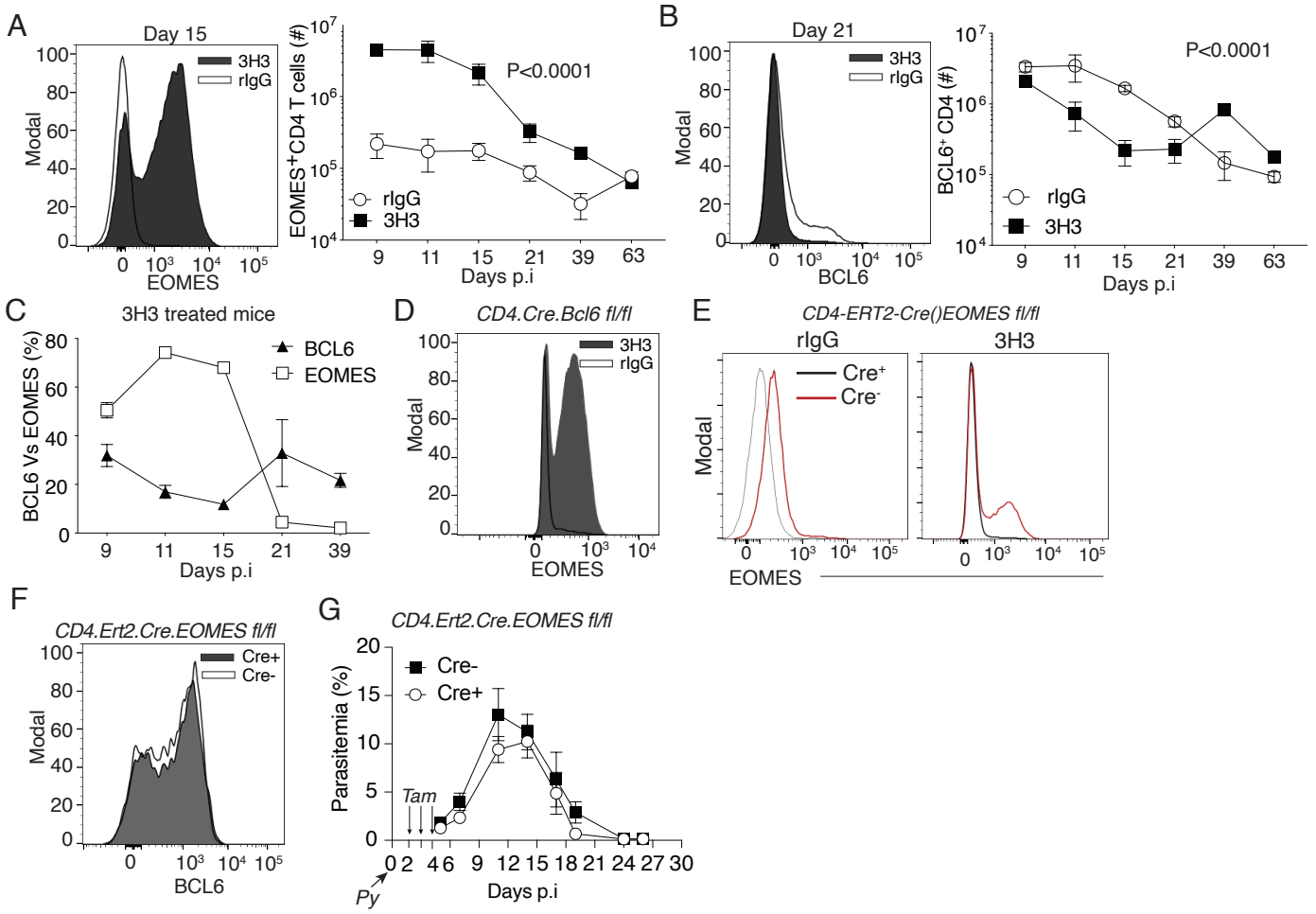

SUPPLEMENTAL FIGURE 2. Representative histograms and kinetics of EOMES (*A*) and BCL6 (*B*) expression in CD4 T cell from *Py*-infected 3H3 or rIgG-treated mice shown. *C*, Relative expression of EOMES and BCL6 in CD4 T cells in *Py*-infected 3H3 mice during the course of infection shown. *D*, Representative histogram of EOMES expression in CD4 T cells in *Py*-infected 3H3 or rIgG-treated *CD4.Cre.Bcl6*$^{fl/fl}$ mice. *E*, Representative histogram showing deletion of EOMES in CD4 T cells in *CD4.Ert2.Cre.Eomes*$^{fl/fl}$ mice treated as in Fig.2. *F*, Representative histogram of BCL6 expression in CD4 T cells in *Py*-infected *CD4.Ert2.Cre.Eomes*$^{fl/fl}$ mice and *G*, kinetics of parasite load in Tam treated *Py*-infected *CD4.Ert2.Cre.Eomes*$^{fl/fl}$ *mice*.

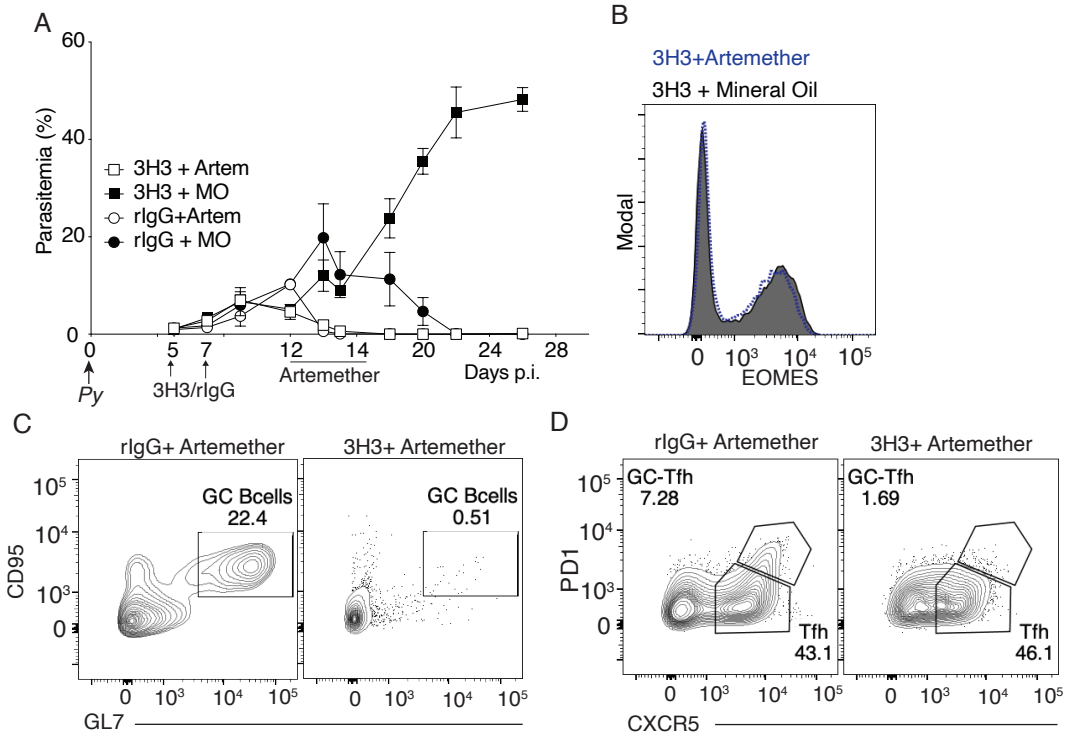

SUPPLEMENTAL FIGURE 3. WT mice were infected with 1x10^6 *Py*-parasitized RBCs and treated with 50 μg of 3H3 or rIgG on days 5 and 7 p.i. and with 100 μL of Artemether (10 mg/mL) on 12-14 dpi and parasite load (*A*), EOMES expression in CD4 T cells (*B*), GC B cells (*C*) and GC-Tfh cells (*D*) measured using flow cytometry.

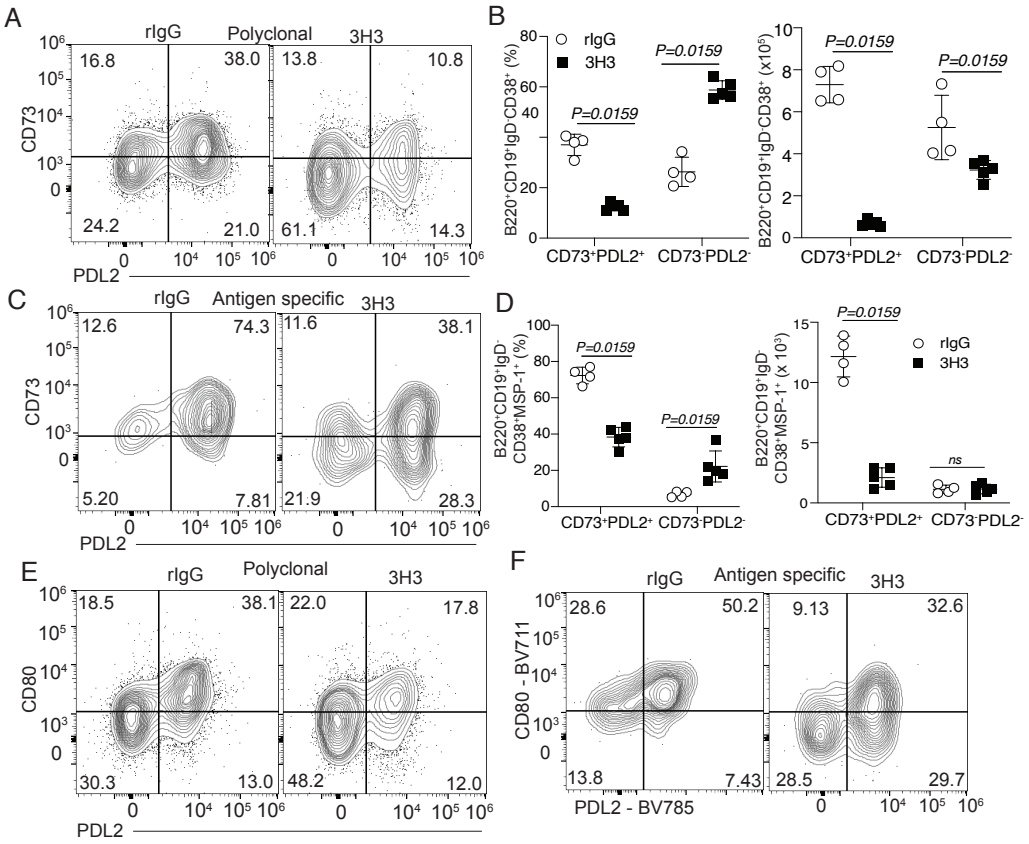

SUPPLEMENTAL FIGURE 4. WT mice were infected with 1x10^6 *Py*-parasitized RBCs and treated with 50 μg of 3H3 or rIgG on days 5 and 7 p.i. were evaluated for different subsets of polyclonal (*A, B, E*) or antigen-specific MBCs (*C, D, F*).